

## Crystal structures and phase transitions in ferromagnetic shape memory alloys based on Co–Ni–Al and Co–Ni–Ga

This article has been downloaded from IOPscience. Please scroll down to see the full text article.

2005 J. Phys.: Condens. Matter 17 1301

(<http://iopscience.iop.org/0953-8984/17/8/008>)

View [the table of contents for this issue](#), or go to the [journal homepage](#) for more

Download details:

IP Address: 129.252.86.83

The article was downloaded on 27/05/2010 at 20:22

Please note that [terms and conditions apply](#).

# Crystal structures and phase transitions in ferromagnetic shape memory alloys based on Co–Ni–Al and Co–Ni–Ga

P J Brown<sup>1,2</sup>, K Ishida<sup>3</sup>, R Kainuma<sup>3</sup>, T Kanomata<sup>4</sup>, K-U Neumann<sup>2</sup>,  
K Oikawa<sup>5</sup>, B Ouladdiaf<sup>1</sup> and K R A Ziebeck<sup>2</sup>

<sup>1</sup> Institut Laue Langevin, BP 156, 38042 Grenoble, France

<sup>2</sup> Department of Physics, Loughborough University, Loughborough LE11 3TU, UK

<sup>3</sup> Department of Materials Science, Graduate School of Engineering, Tohoku University, Sendai 980-8579, Japan

<sup>4</sup> Faculty of Engineering, Tohoku Gakuin University, Tagajo 985, Japan

<sup>5</sup> National Institute of Advanced Industrial Science and Technology, Sendai 938-8551, Japan

Received 13 December 2004, in final form 25 January 2005

Published 11 February 2005

Online at [stacks.iop.org/JPhysCM/17/1301](http://stacks.iop.org/JPhysCM/17/1301)

## Abstract

Magnetization and AC permeability measurements show that the shape memory compounds  $\text{Co}_{1.52}\text{Ni}_{1.32}\text{Al}_{1.16}$  and  $\text{Co}_{1.8}\text{Ni}_{0.92}\text{Ga}_{1.28}$  both order ferromagnetically below  $\approx 280$  K and show a further transition at  $\approx 220$  K. Neutron powder diffraction measurements have confirmed that the lower transition is martensitic and have enabled the structures of the austenite and martensite phases in both compounds to be established. The temperatures at which the transitions occur in the two alloys are similar, as are the structures of both their austenite and martensite phases. The austenite phase of  $\text{Co}_{1.52}\text{Ni}_{1.32}\text{Al}_{1.16}$  is partially ordered in the B2 structure. The martensite phase in both compounds arises from a simple tetragonal distortion of the cubic cell. Unlike the related ferromagnetic shape memory compound  $\text{Ni}_2\text{MnGa}$ , the martensitic transitions are not abrupt and there is a temperature range of at least 100 K in which both tetragonal and cubic phases coexist. The widths of the cubic Bragg peaks are resolution limited but those associated with the tetragonal structure show broadening consistent with the presence of anisotropic micro-strain.

(Some figures in this article are in colour only in the electronic version)

## 1. Introduction

Ferromagnetic shape memory alloys are currently intensively studied because of their potential application as smart materials. The prototype material is  $\text{Ni}_2\text{MnGa}$  in which, however, the martensitic phase transition essential for shape memory behaviour takes place at too low

a temperature for practical applications. The temperature of the transformation  $T_M$  can be increased by changing the stoichiometry; for  $\text{Ni}_{2+x}\text{Mn}_{1-x}\text{Ga}$   $T_M$  reaches the Curie temperature ( $\approx 325$  K) for  $x = 0.19$  [1]. Alloys like  $\text{Ni}_2\text{MnGa}$  with the Heusler alloy structure [2] also tend to be brittle. Recently, new families of ferromagnetic shape memory alloys have been developed based on the  $\beta$  phase in Co–Ni–Al and Co–Ni–Ga ternary alloys [3–7]. In these systems the composition range within which shape memory behaviour occurs is close to the  $\beta(\beta + \gamma)$  phase boundary. The presence of the  $\gamma$  phase, which has the disordered fcc Al structure, is associated with improved ductility. In both systems the temperature  $T_S$  at which the martensitic transformation starts to occur on cooling decreases with increasing Co, Al or Ga content. With decreasing Al or Ga content or increasing Co content both the Curie temperature and the spontaneous magnetization increase. Consequently, by suitable choice of composition and annealing conditions, the transition temperatures and mechanical properties of these ferromagnetic shape memory alloys can be optimized, thus increasing the range of their potential application.

X-ray diffraction measurements on Co–Ni–Al alloys suggest that they transform martensitically from a cubic parent phase with lattice parameter  $a \approx 2.85$  Å to an  $L1_0$  structure with lattice parameters  $a \approx 3.875$  Å and  $c \approx 3.139$  Å [8]. A cubic to tetragonal transformation has also been reported in Co–Ni–Ga alloys, although the lattice parameters given are significantly different with  $a \approx 3.59$  Å for the cubic cell and  $a \approx 2.86$  Å,  $c \approx 2.97$  Å for the tetragonal one [9]. In neither case was a quantitative structural investigation reported. These studies suggest that the martensitic transition leading to shape memory phenomena in the Co–Ni–Al and Co–Ni–Ga systems is qualitatively different from that in  $\text{Ni}_2\text{MnGa}$  and takes place without the development of a super-cell. Precise knowledge of the crystal structures above and below the martensitic transition is important in attempts to understand and to optimize shape memory properties. We have therefore undertaken a neutron powder diffraction investigation, guided by parallel magnetization measurements, of the crystal structures of  $\text{Co}_{1.52}\text{Ni}_{1.32}\text{Al}_{1.16}$  and  $\text{Co}_{1.8}\text{Ni}_{0.92}\text{Ga}_{1.28}$ .

## 2. Sample preparation

100 g samples of  $\text{Co}_{1.52}\text{Ni}_{1.32}\text{Al}_{1.16}$  and  $\text{Co}_{1.52}\text{Ni}_{1.32}\text{Al}_{1.16}$  were prepared by melting the appropriate weights of the spectrographically pure constituent elements (99.9%) in an induction furnace under an argon atmosphere and casting them into metal moulds. Small specimens were cut from the ingots and sealed inside quartz capsules filled with argon gas. The samples were homogenized by heating for one day at 1623 K and for a further day at 1423 K before finally being quenched into ice water. Powders ground from the homogenized samples were sealed in quartz capsules filled with He gas. The powders were annealed to remove strain at 1623 and 1423 K for 20 min and the quartz capsules were then dropped into ice water. Magnetization measurements were made using a SQUID magnetometer in fields of up to 5.5 T and at closely spaced temperatures between 2 and 350 K. The thermal variation of the magnetization of the  $\text{Co}_{1.52}\text{Ni}_{1.32}\text{Al}_{1.16}$  sample measured in fields of 0.1 and 1 T is shown in figure 1(a). There is a clear peak in the magnetization in 0.1 T at approximately 216 K. The derivative of the magnetization shows two anomalies, one at  $\approx 216$  K and the other close to 280 K. Anomalies at these temperatures are also present in the measurements of the initial AC permeability of  $\text{Co}_{1.52}\text{Ni}_{1.32}\text{Al}_{1.16}$ , obtained using an AC transformer method, shown in part (b) of figure 1. Isotherms of magnetization in the form of Arrott plots do not have the linear form expected for isotropic magnets and hence do not give a reliable estimate of the Curie temperature. The lower temperature anomaly showed some hysteresis and so was attributed to a structural phase transition whilst the anomaly at 280 K was identified with the Curie point. The magnetization

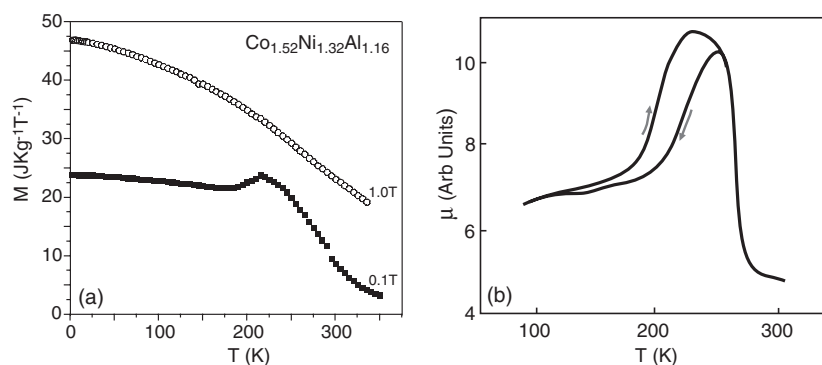


**Figure 1.** The thermal variation in  $\text{Co}_{1.52}\text{Ni}_{1.32}\text{Al}_{1.16}$  of (a) the magnetization in applied fields of 0.1 and 1.0 T and (b) the initial AC permeability  $\mu$ ; the arrows indicate the sense in which the temperature is changing.

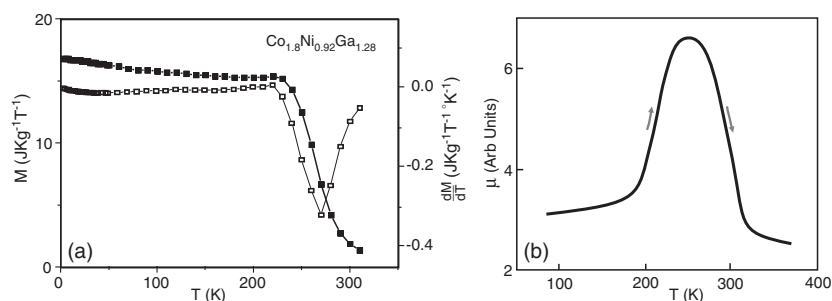


**Figure 2.** (a) The thermal variation of the magnetization of  $\text{Co}_{1.8}\text{Ni}_{0.92}\text{Ga}_{1.28}$ . (a) The magnetization  $\blacksquare$  and its derivative  $\square$  in 0.1 T. (b) The initial AC permeability  $\mu$ ; the arrows indicate the sense in which the temperature is changing.

**Table 1.** Magnetic properties determined for  $\text{Co}_{1.52}\text{Ni}_{1.32}\text{Al}_{1.16}$  and  $\text{Co}_{1.8}\text{Ni}_{0.92}\text{Ga}_{1.28}$ .

Sample	$T_M$ (K)	$T_C$ (K)	$M^a$ ( $\text{J T}^{-1} \text{kg}^{-1}$ )	$\mu$ ( $\mu_B/\text{Co atom}$ )
$\text{Co}_{1.52}\text{Ni}_{1.32}\text{Al}_{1.16}$	216(4)	290(10)	45.4(5)	1.06(3)
$\text{Co}_{1.8}\text{Ni}_{0.92}\text{Ga}_{1.28}$	200(4)	270(5)	38.9(4)	0.97(2)

<sup>a</sup>  $M$  is the magnetization in 5.5 T at 2 K.

in a field of 5.5 T is  $45.4 \text{ J T}^{-1} \text{ kg}^{-1}$  at 2 K, which corresponds to a moment of  $0.40 \mu_B/\text{atom}$  or  $1.06 \mu_B/\text{Co atom}$ .

The low field (0.1 T) magnetization of  $\text{Co}_{1.8}\text{Ni}_{0.92}\text{Ga}_{1.28}$ , shown in figure 2(a), begins to decrease at temperatures greater than  $\approx 220$  K. The derivative with respect to temperature has a single anomaly around 270 K which was assumed to be the Curie temperature. This identification was confirmed by the AC transformer measurements of the initial permeability shown in figure 2(b). The magnetization in a field of 5.5 T is  $38.9 \text{ J T}^{-1} \text{ kg}^{-1}$  at 2 K which corresponds to  $0.435 \mu_B/\text{atom}$  or  $0.97 \mu_B/\text{Co atom}$ . The results obtained from the magnetization measurements on both alloys are summarized in table 1.

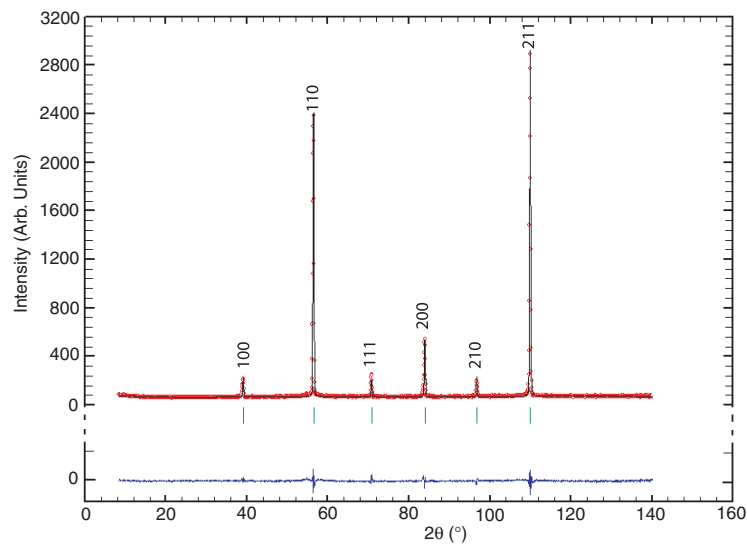


**Figure 3.** The neutron powder diffraction pattern of  $\text{Co}_{1.52}\text{Ni}_{1.32}\text{Al}_{1.16}$  at 450 K. The plotted points show the observed counts and the full curve is the calculated profile. The inset at the bottom is the difference between the observed and calculated patterns. The calculated positions of the reflections are shown as vertical lines.

### 3. Neutron diffraction

Neutron powder diffraction measurements were carried out using the high resolution diffractometer D1A at the Institut Laue Langevin in Grenoble. The powder samples were contained in thin walled vanadium cans mounted inside an ILL cryo-furnace which allowed them to be maintained at temperatures between 2 and 500 K. Diffraction patterns were recorded at temperatures between 5 and 450 K using a neutron wavelength  $1.911 \text{ \AA}$  and steps of  $0.05^\circ$  in scattering angle from  $1^\circ$  to  $160^\circ$ . The diffraction patterns were analysed using the FULLPROF profile refinement package [10]. A statistical  $\chi^2$  test was used to measure the goodness of the fits obtained in the profile refinements; it is defined by

$$\chi^2 = \frac{\sum_{\text{observations}} ((I_o - I_c) / \sigma I_o)^2}{N_o - N_p} \quad (1)$$

where  $I_o$  and  $I_c$  are the observed and calculated intensities for the  $N_o$  measured points,  $\sigma I_o$  is the estimated standard deviation of  $I_o$ , and  $N_p$  is the number of fitted parameters.

#### 3.1. $\text{Co}_{1.52}\text{Ni}_{1.32}\text{Al}_{1.16}$

The neutron powder diffraction pattern obtained from  $\text{Co}_{1.52}\text{Ni}_{1.32}\text{Al}_{1.16}$  at 450 K is shown in figure 3. At this temperature the alloy is in the paramagnetic state  $T_C \approx 270 \text{ K}$ . Six distinct Bragg peaks can be seen in the angular range  $8^\circ$ – $140^\circ$ ; they can all be indexed using a primitive cubic unit cell  $a = 2.857 \text{ \AA}$ . This shows that the sample is a single phase which is partially ordered in the B2 structure so that super-lattice reflections with  $h + k + l$  odd occur. A profile refinement was carried out, based on these parameters in which the site occupancies were allowed to vary. This enabled the relative scattering lengths of the corner and body centre sites to be determined. The fit obtained,  $\chi^2 = 4.18$ , was reasonable but the intensity of the 211 Bragg peak was slightly underestimated. The results are given in table 2 and the calculated and observed profiles in figure 3. The diffraction pattern recorded at 270 K was similar to that

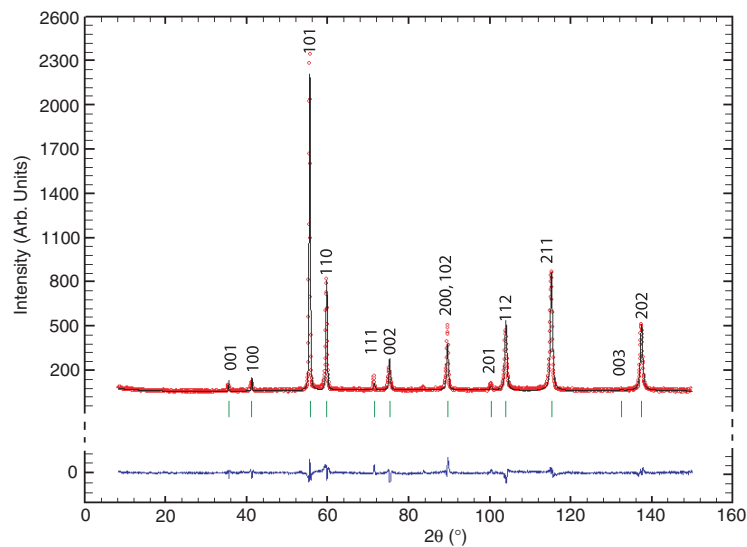


**Figure 4.** The neutron powder diffraction pattern of  $\text{Co}_{1.52}\text{Ni}_{1.32}\text{Al}_{1.16}$  at 10 K, displayed in the same way as figure 3.

**Table 2.** Crystal structures of  $\text{Co}_{1.8}\text{Ni}_{0.92}\text{Ga}_{1.28}$  and  $\text{Co}_{1.52}\text{Ni}_{1.32}\text{Al}_{1.16}$  alloys determined by neutron powder diffraction.

$T$ (K)	Structure	Lattice ( $\text{\AA}$ )	Volume ( $\text{\AA}^3$ )	$B$ ( $\text{\AA}^2$ )	Site b (fm)	$\sigma^a \times 10^4$	$\chi^2$
$\text{Co}_{1.8}\text{Ni}_{0.92}\text{Ga}_{1.28}$							
350	$A2\ I\bar{m}\bar{3}m$	$a = 2.8720$	23.6894(6)	0.80(4)	2a		2.1
	$A2\ I\bar{m}\bar{3}m\ 30\%$	$a = 2.8657(2)$	23.5338(6)	0.88(4)	2a		
200	$I4/mmm\ 70\%$	$a = 2.7489(1)$ $c = 3.1151(2)$	23.5391(6)	0.88(4)	2a	$\sigma_a = 21(3)$ $\sigma_c = 38(4)$	1.5
$\text{Co}_{1.52}\text{Ni}_{1.32}\text{Al}_{1.16}$							
450	$B2\ P\bar{m}\bar{3}m$	$a = 2.8571(2)$	23.3226(6)	0.95(4)	1a 6.91(1) 1b 3.85(1)		4.2
10	$B2\ P4/mmm$	$a = 2.7139(1)$ $c = 3.1311(2)$	23.3226(6)	0.60(4)	1a 6.39(1) 1b 4.37(1)	$\sigma_a = 27(4)$ $\sigma_c = 35(4)$	2.0

<sup>a</sup> Micro-strains determined from line broadening.

observed at 450 K apart from a single very weak additional peak with  $2\theta \approx 90^\circ$  and intensity less than 1% of the cubic fundamental reflections. On further cooling to 235 K the cubic phase remains predominant, but two very small extra peaks which could be associated with a tetragonal distortion of the cubic cell were just visible. At 210 K, 60% of the sample has transformed to a tetragonal martensitic phase with cell parameters  $a = 2.736\ \text{\AA}$ ,  $c = 3.089\ \text{\AA}$ . At 10 K (figure 4) the transformation to the tetragonal structure is complete. The variation of lattice constants is shown in figure 8. Although there is a discontinuity in lattice constant at the transition the cell volume remains nearly constant.

### 3.2. $\text{Co}_{1.8}\text{Ni}_{0.92}\text{Ga}_{1.28}$

The neutron powder diffraction pattern of  $\text{Co}_{1.8}\text{Ni}_{0.92}\text{Ga}_{1.28}$  obtained in the austenite phase at 350 K is shown in figure 5. Only four Bragg peaks occur in the angular range  $2\theta = 8^\circ\text{--}140^\circ$

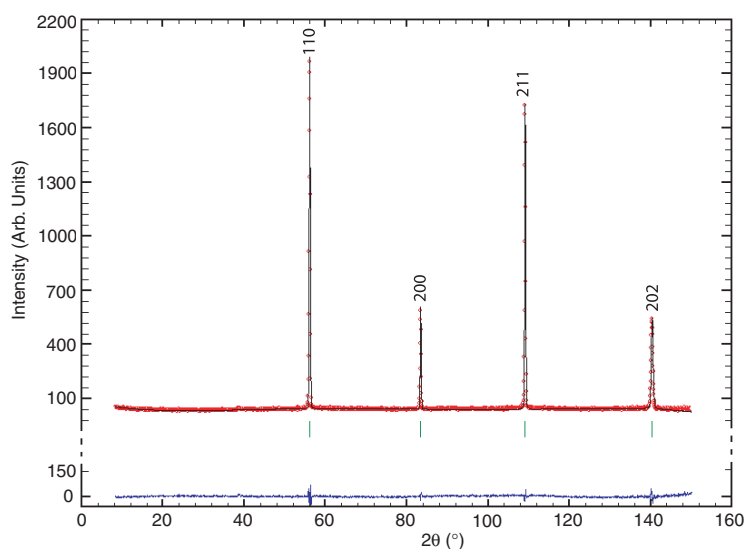


**Figure 5.** The neutron powder diffraction pattern of  $\text{Co}_{1.8}\text{Ni}_{0.92}\text{Ga}_{1.28}$  at 350 K, displayed in the same way as figure 3.

covered in the experiment. These peaks can be indexed on a bcc lattice, confirming that the sample is single phase. No reflections with  $h+k+l$  odd which would indicate B2 type ordering are visible. Profile refinement of the diffracted intensities confirmed the structure and showed that the difference between the scattering lengths at the corner and body-centre sites is less than  $\approx 0.5$  fm.

The powder pattern was essentially unchanged on cooling to 250 K although the value of  $\chi^2 = 4.8$  obtained from the profile refinement was significantly greater than that obtained with the 350 K data. This was traced to a 2% underestimate of the calculated intensity of the 211 reflection. A refinement allowing a small degree of preferred orientation in the 211 direction gave an improved  $\chi^2 = 2.25$ . The pattern obtained at 200 K shown in figure 6 is more complex; the four bcc reflections have split showing that the cubic symmetry is lost. The new peaks can be indexed on a body centred tetragonal cell with  $a = 2.7492$  Å and  $c = 3.1156$  Å; the four reflections belonging to the original cubic cell are still present but with a much reduced intensity. Comparison of the intensities of the cubic peaks at 200 and 350 K showed that at 200 K 30% of the sample remained in the cubic phase. The only significant change in the diffraction patterns recorded on cooling to 150 and then to 10 K was in the intensity of the cubic peaks; this indicated that at 150 K 90% of the sample had transformed to the tetragonal phase. At 10 K, the lowest temperature at which measurements were made, only about 1% of the cubic phase remained. A refinement using the 200 K data was carried out based on a model containing both tetragonal and cubic phases. This model accounted for all the observed reflections but gave a rather poor  $\chi^2 = 8.5$ . Although agreement between the observed and calculated intensities for the cubic component was excellent, there were significant differences associated with the tetragonal peaks.

### 3.3. Peak shape analysis

Examination of the peak profiles in the powder pattern of  $\text{Co}_{1.8}\text{Ni}_{0.92}\text{Ga}_{1.28}$  recorded at 200 K showed that whilst the shapes of the cubic peaks were essentially the same as those observed

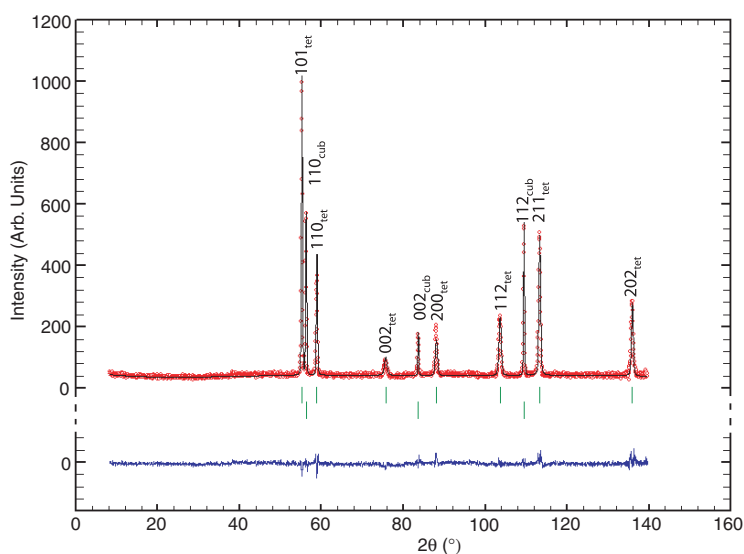


**Figure 6.** The neutron powder diffraction pattern of  $\text{Co}_{1.8}\text{Ni}_{0.92}\text{Ga}_{1.28}$  at 200 K, displayed in the same way as figure 3.

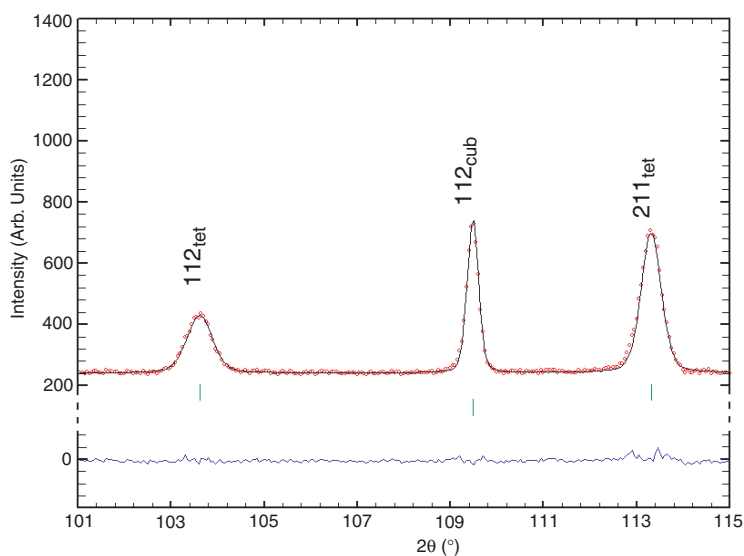


**Figure 7.** The shapes of the 211 peaks in the neutron powder diffraction pattern of  $\text{Co}_{1.8}\text{Ni}_{0.92}\text{Ga}_{1.28}$  at 200 K, showing the fit obtained by including broadening due to micro-strain in the profile refinement.

at 350 K, the tetragonal reflections were anomalously broader. The width of the tetragonal peaks increased with scattering angle but with some systematic fluctuation. Reflections with non-zero  $l$  were systematically broader than those of the form  $hk0$ . The shapes of the group of three peaks derived from the cubic  $\{112\}$  planes and recorded at 200 K are compared in figure 7. Between 200 and 10 K the widths of the Bragg peaks remain essentially unchanged, suggesting that the line broadening is introduced at the martensitic transition and undergoes no further evolution.



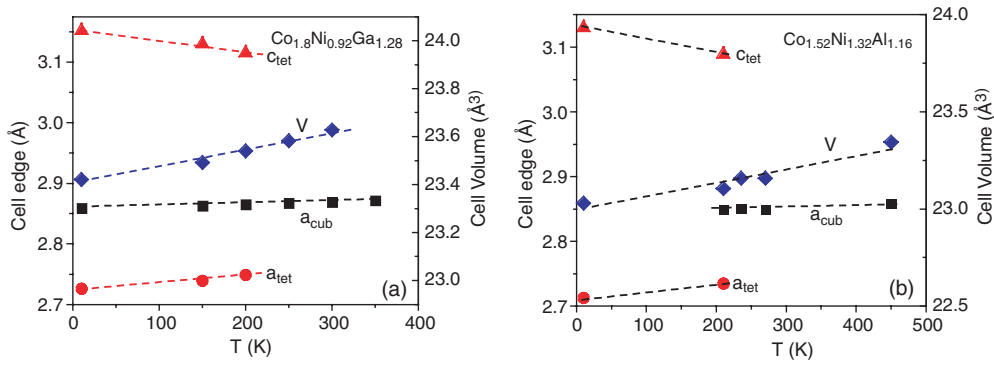


**Figure 8.** The thermal variation of the lattice parameters and cell volume in (a)  $\text{Co}_{1.8}\text{Ni}_{0.92}\text{Ga}_{1.28}$  and (b)  $\text{Co}_{1.52}\text{Ni}_{1.32}\text{Al}_{1.16}$ .

The shape of the Bragg peaks in a powder pattern is given by the convolution of the instrumental resolution with the intrinsic peak shape due to the sample. The intrinsic shape is determined by particle size, sample uniformity and in particular by residual strain. The peaks due to the cubic phase of  $\text{Co}_{1.8}\text{Ni}_{0.92}\text{Ga}_{1.28}$  have a Gaussian shape and a width, which is resolution limited. Owing to the resolution characteristics of the diffractometer D1A, their shape does not change substantially over the angular range  $30^\circ$ – $120^\circ$ . The broadening of the tetragonal reflections which develop in the phase transition can be attributed to micro-strains leading to fluctuations in the lattice parameters of the tetragonal phase. Within the FULLPROF programme provision is made for analysing the broadening of reflections by micro-strains using the variance of the reflection widths [11, 12]. The variance is related to a general strain tensor, the elements of which are restricted by symmetry. Although at  $T_M$  there is a large change in lattice parameter  $c_{\text{tet}}/a_{\text{cub}} \approx 1.13$ , it may be seen from figure 8 that there is negligible variation in cell volume. Single-crystal measurements show that the analogous phase transition in  $\text{Ni}_2\text{MnGa}$  occurs via shears in (110) planes [13]. When the linear strain of the transformation is  $\sigma$ , the transformed tetragonal cell has parameters  $a_{\text{tet}} = a_{\text{cub}}(1 - \sigma)$  and  $c_{\text{tet}} = a_{\text{cub}}(1 + 2\sigma)$  with  $\sigma \approx 0.042$ . If the same mechanism is responsible for the transition in  $\text{Co}_{1.8}\text{Ni}_{0.92}\text{Ga}_{1.28}$  then the strains in the  $a$ – $b$  plane and along  $c$  will be correlated. A refinement was carried out in which uncorrelated Gaussian distributions of strains along both  $a$  and  $c$  axes were included. The instrumental resolution function used for the refinement of the tetragonal phase was fixed to that determined for the cubic component. The  $\chi^2$  value obtained for this refinement was 1.51 and the observed and calculated profiles are in good agreement as shown in figure 7. The parameters characterizing the micro-strain are  $\sigma_a = 21(3) \times 10^{-4}$  and  $\sigma_c = 38(4) \times 10^{-4}$  for the  $a$  and  $c$  parameters respectively. Within experimental error  $\sigma_c = 2\sigma_a$  in accordance with the shear mechanism proposed above. The full results of the refinement are given in table 2. In a subsequent refinement a ferromagnetic moment of  $0.783 \mu_B/\text{cobalt atom}$ , as determined from the bulk magnetization, was included in the model. This addition did not improve the quality of the fit.

The width of the cubic reflections for  $\text{Co}_{1.52}\text{Ni}_{1.32}\text{Al}_{1.16}$  were similar to those observed for  $\text{Co}_{1.8}\text{Ni}_{0.92}\text{Ga}_{1.28}$  and did not change significantly with temperature. On the other hand, as for  $\text{Co}_{1.8}\text{Ni}_{0.92}\text{Ga}_{1.28}$ , the tetragonal peaks are significantly broader and their widths do not change on cooling below  $T_M$ . Although broadening was observed in both alloys, that present in  $\text{Co}_{1.52}\text{Ni}_{1.32}\text{Al}_{1.16}$  was less anisotropic with  $hh0$  and  $00l$  reflections having similar widths. A profile refinement similar to that done for the transformed phase of  $\text{Co}_{1.8}\text{Ni}_{0.92}\text{Ga}_{1.28}$

was carried out using the data collected at 10 K. The results are given in table 2. Again no improvement in the quality of the fit was obtained by including the ferromagnetic moment.

#### 4. Conclusions

Neutron diffraction measurements show that, when annealed at temperatures above 1400 K and then quenched, the ferromagnetic shape memory alloys  $\text{Co}_{1.52}\text{Ni}_{1.32}\text{Al}_{1.16}$  and  $\text{Co}_{1.8}\text{Ni}_{0.92}\text{Ga}_{1.28}$  both consist of a single phase which has cubic symmetry at temperatures above 270 K and transforms to a tetragonal phase on cooling. The lattice parameters determined for both the cubic and tetragonal phases of  $\text{Co}_{1.8}\text{Ni}_{0.92}\text{Ga}_{1.28}$  are significantly different from those reported previously from x-ray measurements [9]. There is better agreement with the x-ray measurements for  $\text{Co}_{1.52}\text{Ni}_{1.32}\text{Al}_{1.16}$  [8]. The austenite phase of  $\text{Co}_{1.52}\text{Ni}_{1.32}\text{Al}_{1.16}$  is partially ordered in the B2 structure but the presence of three constituents does not allow a unique solution for the atomic order. The  $\beta$  phases NiAl and CoAl both order with the B2 structure so it is most likely that in the ternary alloys one of the sites is occupied preferentially by Ni and Co and the other by Al and the surplus transition metal atoms. If this ordering were complete the site scattering lengths would be 6.11 and 4.57 fm respectively. The slightly more disparate values observed suggest that the additional disorder is between Al and Co. If this type of order were present in  $\text{Co}_{1.8}\text{Ni}_{0.92}\text{Ga}_{1.28}$  the difference in the site scattering lengths would be only  $\approx 0.4$  fm and so the absence of the  $h + k + l$  odd peaks in the powder patterns does not preclude partial B2 order.

The present experiments have shown that the magnetic properties, structures and transformation temperatures in the alloys  $\text{Co}_{1.52}\text{Ni}_{1.32}\text{Al}_{1.16}$  and  $\text{Co}_{1.8}\text{Ni}_{0.92}\text{Ga}_{1.28}$  are very similar. All the Bragg peaks observed in the temperature range covered in the experiments could be associated with either the simple cubic or the simple tetragonal cell. Thus the transition from the cubic austenite to the tetragonal martensite appears to take place without the intermediate step of a premartensitic phase such as that which occurs in  $\text{Ni}_2\text{MnGa}$  [14]. Some evidence of an impending phase transition may be inferred from the small increase in the intensity of the cubic 211 reflection observed in  $\text{Co}_{1.8}\text{Ni}_{0.92}\text{Ga}_{1.28}$  at 250 K and from the very weak extra peak observed in  $\text{Co}_{1.52}\text{Ni}_{1.32}\text{Al}_{1.16}$  at 270 K.

The martensitic transition in these two Co–Ni based alloys is not abrupt, as it is in  $\text{Ni}_2\text{MnGa}$ , but takes place over a broad temperature interval in which both cubic and tetragonal phases coexist. In  $\text{Co}_{1.8}\text{Ni}_{0.92}\text{Ga}_{1.28}$  some cubic phase is still present at temperatures more than 200 K below  $T_M$ , a very small fraction remaining even at 10 K. For  $\text{Co}_{1.52}\text{Ni}_{1.32}\text{Al}_{1.16}$  the range of coexistence of the two phases is significantly smaller,  $\approx 100$  K, and at 10 K only the tetragonal phase is present. In both alloys the widths of the diffraction peaks from the martensitic phase give evidence for the presence of micro-strain in the transformed phase. These micro-strains which measure the spread in the shear strain characterizing the transition are an order of magnitude smaller than the strain arising from the deformation itself ( $\sigma \approx 0.42$ ). Either or both of these properties which distinguish the Co–Ni based alloys from the brittle  $\text{Ni}_2\text{MnGa}$  system may be associated with their improved ductility.

#### References

- [1] Vasilèv A N, Bozhko A D, Khovailo V V, Dikshtein I E, Shavrov V G, Buchelnikov V D, Matsumoto M, Suzuki S, Takagi T and Tani J 1999 *Phys. Rev. B* **59** 1113
- [2] Webster P J, Ziebeck K R A, Town S L and Peak M S 1984 *Phil. Mag.* **49** 295
- [3] Chernenko V A, Pons J, Cesari E and Zaslachuk I K 2004 *Scr. Mater.* **50** 225
- [4] Oikawa K, Ota T, Gejima F, Ohmori T, Kainmura R and Ishida K 2001 *Mater. Trans. JIM* **42** 2472

- 
- [5] Oikawa K, Wulff L, Iijima T, Gejima F, Ohmori T, Fujita A, Fukamichi K, Kainuma R and Ishida K 2001 *Appl. Phys. Lett.* **79** 3290
  - [6] Wuttig M, Li J and Craciunescu C 2002 *Scr. Mater.* **44** 2393
  - [7] Craciunescu C, Kishi Y, Lograsso T A and Wuttig M 2002 *Scr. Mater.* **47** 285
  - [8] Oikawa K, Omori T, Sutou Y, Kainuma R and Ishida K 2003 *J. Physique* **112** 1017
  - [9] Sato M, Okazaki T, Furuya Y and Wuttig M 2003 *Mater. Trans.* **44** 372
  - [10] Rodriguez-Carvajal J 1997 *FULLPROF Version 3.3* Laboratoire Leon Brillouin
  - [11] Rodriguez-Carvajal J, Fernández-Díaz M T and Martínez J L 1993 *J. Phys.: Condens. Matter* **3** 3215
  - [12] Stephens P W 1999 *J. Appl. Crystallogr.* **32** 281
  - [13] Brown P J, Dennis B, Crangle J, Kanomata T, Matsumoto M, Neumann K-U, Justham L M and Ziebeck K R A 2004 *J. Phys.: Condens. Matter* **16** 65
  - [14] Brown P J, Crangle J, Kanomata T, Matsumoto M, Ouladdiaf B, Neumann K-U and Ziebeck K R A 2002 *J. Phys.: Condens. Matter* **14** 10159